



encit 2020



18<sup>th</sup> Brazilian Congress of Thermal Sciences and Engineering  
November 16-20, 2020 (Online)

ENC-2020-0117

## EXPERIMENTAL EVALUATION OF THE CONVECTIVE CONDENSATION HEAT TRANSFER COEFFICIENT INSIDE A HORIZONTAL CONVENTIONAL-SIZED CHANNEL

Tiago Augusto Moreira

Gherhardt Ribatski

Heat Transfer Research Group – HTRG, Department of Mechanical Engineering, São Carlos School of Engineering (EESC), University of Sao Paulo (USP), 400 Trabalhador São-Carlense Ave., Parque Arnold Schmidt, ZIP code: 13566-590, São Carlos, SP, Brazil.

tiago.moreira@usp.br

ribatski@sc.usp.br

**Abstract.** *In commercial, domestic and industrial refrigeration applications the largest amount of mass inside the system is verified at the condenser. Therefore, attention should be given to the optimization of such component focusing on the reduction of the refrigerant load associated to the increase of the system efficiency. Such optimization is achieved using accurate prediction methods for the heat transfer coefficient, which development rely in extensive databases due to their semi-empirical nature. In the present study, experiments for the convective condensation heat transfer coefficient were performed in a 9.43 mm inner diameter channel for the R134a. Data was obtained at a saturation temperature of 35°C with mass velocity varying from 100 to 400 kg/m<sup>2</sup>s, heat fluxes from 10 to 40 kW/m<sup>2</sup> and vapor qualities up to the unity. In general, the heat transfer coefficient increases with increasing mass velocity and vapor quality (except for  $G=100$  kg/m<sup>2</sup>s). A negligible effect of heat flux was verified for all mass velocities. The results were compared against prediction methods available in the literature, showing reasonable agreement.*

**Keywords:** *heat transfer coefficient, convective condensation, two-phase flow*

### 1. INTRODUCTION

In refrigeration systems the correct design of heat exchangers is essential to increase its efficiency and reduce refrigerant charge (Khuen, 1998). As the largest amount of fluid in the circuit is present in the condenser, focus should be given to it. To optimize this component, accurate and reliable prediction methods for the heat transfer coefficient ( $HTC$ ) and pressure drop are necessary, which development depends on data for a broad range of experimental conditions.

Recently, due to the phase-out of HFCs and HCFCs set to occur in 2045 for countries under development, such as Brazil, by the Kigali amendment (2016) to the Montreal Protocol, studies have focused on evaluating the convective condensation performance of low GWP (Global Warming Potential) and null ODP (Ozone Depletion Potential) fluids, such as HFOs and hydrocarbons (Macdonald and Garimella 2016a; Sempertégui-Tápia and Ribatski, 2017; Longo et al., 2017; Fries et al, 2018, Longo et al., 2019). However, the use of fluids like R134a will remain for more than two and half decades. With the aim to reduce their impact on the environment during this period, optimized systems are required to minimize the use (charge) of such refrigerant. Therefore, the experimental evaluation of the convective condensation heat transfer coefficient and the performance of prediction methods is still necessary.

In this context, the present paper concerns an experimental evaluation of the heat transfer coefficient during convective condensation of R134a in a horizontal tube. The experiments were conducted for mass velocities ranging from 100 to 400 kg/m<sup>2</sup>s, heat fluxes from 10 to 40 kW/m<sup>2</sup>s and vapor qualities up to the unity. The data were compared against twenty prediction methods from literature.

### 2. EXPERIMENTAL RIG

The experimental rig, schematically illustrated in Fig. 1, was built to perform experiments for flow boiling and convective condensation using a secondary fluid, and for flow boiling using electric heaters. Since the present study concerns an investigation on condensation, the components of the test-loop associated to evaporation tests using electric heating are not used and, therefore, not described in this text. For further details of them, the following references are recommended Kanizawa (2011), Mogaji (2014) and Ayub et al. (2017).

In the facility, the fluid is driven through the circuit by a gear oil-free micropump (A for high mass fluxes, micropump GD 223/56C, and B for low mass fluxes, micropump GC M23 JKS5). Upstream the micropumps there are the condenser and the filter-dryer. A Coriolis type mass flow meter located just downstream the micropumps is used to evaluate the refrigerant mass flow rate. Between the mass flow meter and the pre-heater, the test fluid flows through a tube-in-tube sub-cooler to ascertain the absence of vapor bubbles within the refrigerant. Thereby, the thermodynamic state of the refrigerant at the pre-heater inlet can be evaluated based on the temperature and pressure measurements, see Fig. 1. The sub-cooler is supplied by a cooling water+EG secondary circuit.

Posterior to the sub-cooler, by manipulating ball valves just downstream a T-junction (see Fig. 1), the operating circuit is set either electric heating or counter-current water as heat transfer source. According to the last mode, for water as heat transfer source, the valves arrangement to operate are the following (see Fig. 1): (i) opened: 4 (or 5) 6, 10, 11, 13 and 14; (ii) closed: 2, 3, 7, 8, 9, 15, 16, 17 and 18; and (iii) partially opened: 12 and 19. All the valves in the circuit are ball valves (diameter of 1/2") manufactured by Swagelok Co., except for valve 19, which is a needle type produced by the same company. Valves 12 and 19 operates partially opened and are used to help to control the pressure and, consequently, the temperature of the working fluid at the test section.

The pre-heater consists of a tube-in-tube heat exchanger, with the inner tube made of stainless steel and the outer of chlorinated polyvinyl chloride (CPVC). The internal diameters of the inner and outer tubes are 11.3 and 23.7 mm, respectively, and their total lengths are 8 m. The refrigerant flows inside the inner tube and hot water flows counter-currently to the refrigerant in the annuli. Temperature and pressure measurements are performed at the inlet and outlet sections of the refrigerant side, and water temperature is evaluated at the pre-heater inlet and outlet sections. A flow calming section is located downstream the pre-heater designed to guarantee hydraulic developed flow at the test section entrance.

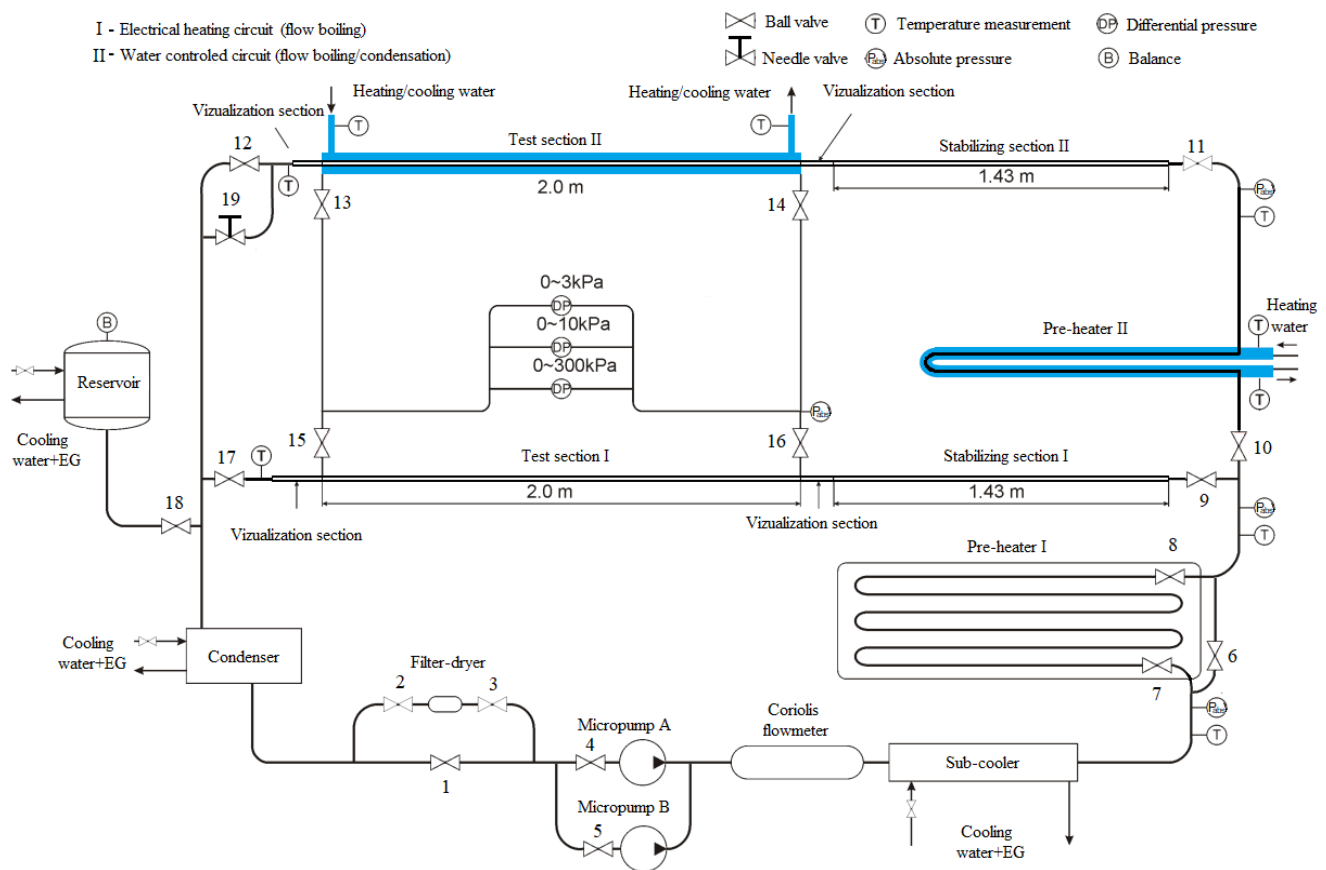


Figure 1. In-tube refrigerant loop schematic

The test section is comprised of two stainless steel tubes assembled one inside the other. The inner tube is 9.43 mm ID and 13.63 mm OD, and the outer is 18 mm ID and 22.14 mm OD. Figure 2 illustrates a schematic of test section. As it can be seen, water temperature measurements are performed through thermistors from Fluke Corp. with high accuracy (smaller than 0.01°C) at the inlet and outlet, and by thermocouples in 4 cross-sections equally spaced along the tube. At each cross-section four water temperature measurements are performed in order to reduce the uncertainty of the measurements. In each measurement section, besides the water temperature, data are acquired for the temperature of the refrigerant and for the inner tube wall, as illustrated in Fig. 2. In this figure it is possible to observe the disposition

of the thermocouples in each measurement section. The pressure drop across the test section length is measured through one of the three differential pressure transducers (see Fig. 1). Three differential pressure transducers with measurement ranges of 0-3, 0-10 and 0-300 kPa are used to minimize the uncertainty of the pressure drop measurements. Temperature measurements along the loop made through thermocouples uses K-type ones with hot junction diameter of 0.254 mm from Omega Inc. A condenser is located downstream the test section to condense the remaining vapor from the test section and sub-cool the test fluid. It consists of a shell-and-tube heat exchanger with the refrigerant flowing at the shell side and the anti-freezing solution (same of the sub-cooler) in the tubes side. To record the data and to monitor and control the experimental apparatus, a National Instruments data acquisition system (chassis SCXI-1000 associated to the modules SCXI-1303, SCXI-1302 and SCXI-1112) with a LabView program were used.

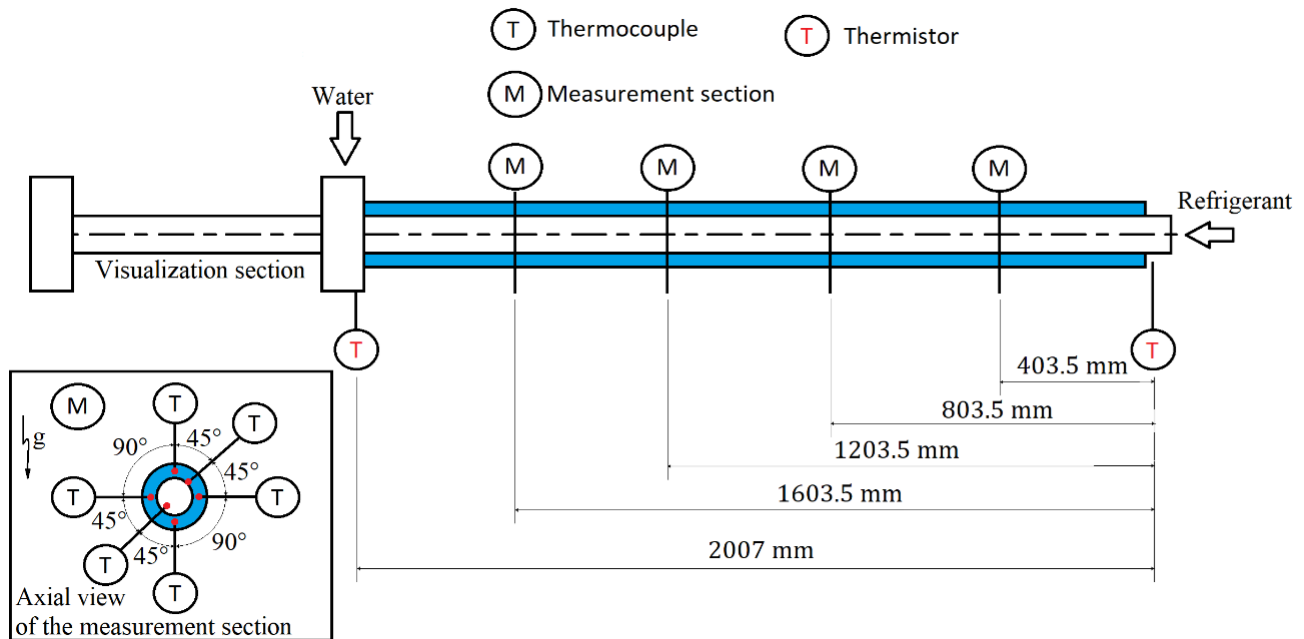


Figure 2. Test section schematic

## 2.1 Data regression procedure

The mass velocity of the refrigerant inside the test section is calculated as the ratio between the mass flow rate, evaluated through the Coriolis mass flow meter, and the inner cross-sectional area of the test section. The thermodynamic condition of the fluid at the inlet of the test section is determined based on an energy balance over the pre-heater, discounting the heat losses to the environment. To estimate the heat losses along the pre-heater, tests were performed for hot water flowing in the annuli region with vacuum condition established in the inner tube (refrigerant side). Then, based on the inlet and outlet water temperatures and water mass flow rate, evaluated by a magnetic flow meter (Rosemount, model 8711), the heat losses were estimated through energy balances over the pre-heater and correlated to the difference among the average water temperature and environmental one. For the heat losses (or heat gains, depending on the difference between the temperature of the water and environment) at the test section, similar procedure than the one used for the pre-heater was adopted, once that inlet and outlet temperatures are known through the thermistors and the water mass flow rate evaluated in a similar magnetic flow meter.

It is worth to highlight that the magnetic flow meters positioned on the heating/cooling and heating water circuits evaluate only the volumetric flow rate. To obtain the water mass flow rate in each circuit, the value measured through the magnetic flow meters is multiplied by the local density of the water. In the heating water circuit, the magnetic flow meter is positioned downstream the pre-heater, and in the heating/cooling water circuit downstream the test section. Therefore, the temperature used to evaluate the density of the water at the magnetic flow meters are the ones corresponding to the outlet of the pre-heater for the heating water circuit, and outlet of the test section for the heating/cooling water circuit.

The vapor quality at each measurement section and at the outlet of the test tube were estimated based on local energy balances discounting the heat losses to the environment from the total heat transferred to both water and environment. The heat losses between the measurement sections were calculated as a ponderation considering the total heat loss and test section length.

The heat transfer coefficient, *HTC*, is calculated according to the Newton's cooling law considering the effects of radial conduction through the test tube wall, as it follows:

$$\frac{1}{HTC} = \frac{T_{wall,i} - T_f}{q_{local}} - \frac{d_{int} \ln\left(\frac{(d_{ext} - 2e_h)/d_{int}}{d_{int}}\right)}{2k_t} \quad (1)$$

where  $k_t$  is the thermal conductivity of the test tube wall,  $T_{wall,i}$  the inner tube wall temperature,  $T_f$  the working fluid temperature (directly measured by positioning a thermocouple in a bulb within the flow),  $d_{int}$  and  $d_{ext}$  the internal and external diameters of the inner tube, respectively,  $e_h$  the deepness of the hole used to assemble the thermocouple in the test tube (1.7 mm) and  $q_{local}$  the local heat flux, estimated by the following:

$$q_{local} = \frac{m_w c_{p,w}}{\pi d_{int}} \left( \frac{dT_w}{dz} \right)_{z=z_1} \quad (2)$$

where  $m_w$ ,  $T_w$  and  $c_{p,w}$  are the water mass flow rate, temperature and specific heat, respectively,  $z$  the length along the test tube according to the axial direction and  $z_1$  an specific location along it. The water temperature at each measurement cross-section is given as the arithmetic average of the four thermocouples positioned within the water flow (see Fig. 2). In order to account for the heat losses on the calculus of the heat flux, the amount of heat lost estimated according to procedure previously mentioned in this section was pondered according to the distance from the outlet of the test section (the water flows counter-current to the fluid) and discounted from the water temperature measurements through energy balances. A second order polynomial as function of the distance along the test section was then adjusted to obtain the derivative of the water temperature profile,  $dT_w/dz$ , using procedure employed by Del Col et al. (2011) (weighted least square regression method).

## 2.2 Uncertainty evaluation

Temperature measurements performed through the thermocouples, except for the ones assembled to the test section, were calibrated using a thermal bath (Haake AC200-A40) associated with a precision thermometer (FLUKE-1523-P1 reference thermometer, probe 5616 PRT, uncertainty of 0.011°C). The calibration of the thermocouples fixed along the test section was performed *in loco* by flowing water, which temperature was controlled through the same thermal bath above-mentioned, in the annuli at high Reynolds numbers using a centrifugal pump (Mark NXDP-2, 0.5 cv). In this case, the reference temperature was assumed as the average among the values measured at the inlet and outlet of the test section through the thermistors (the difference between these measurements was always below 0.02°C). In both thermocouples' calibration setups, the uncertainties were evaluated according to the procedure suggested by Abernethy and Thompson (1973). Similar calibration procedures were adopted for the absolute and differential pressure transducers, using as reference a pressure indicator model CPG 2500 from WIKA (0-2000 kPa, accuracy of 0.08 kPa). The uncertainty of the measurements provided by the manufacturer were adopted for the magnetic flow meters, Coriolis mass flowmeter and the thermistors. The uncertainty propagation procedure presented Taylor and Kuyatt (1994) was used to estimate the heat transfer coefficient uncertainty, which showed a mean value of 6% of the measured value. The procedure suggested by Del Col et al. (2011) was adopted to account for the uncertainty in the estimative of  $dT_w/dz$ .

## 2.3 Validation

To validate the experimental rig and the data regression procedure, single-phase flow experiments for the heat transfer coefficient were performed and the results compared against the prediction methods by Gnielinki (1976) and Dittus and Boelter (1930). Figure 3 illustrates the comparison between the experimental data and the values predicted by these methods with varying Reynolds number. As noted in this figure, a reasonable agreement was obtained, validating the experimental rig and data regression procedures.

## 3. RESULTS

Convective condensation experiments were performed for R134a at a saturation temperature of 35±1°C, mass velocities ranging from 100 to 400 kg/m<sup>2</sup>s, heat fluxes from 10 to 40 kW/m<sup>2</sup> and vapor qualities up to the unity. Figure 4 illustrates the behavior of the heat transfer coefficient with varying vapor quality at  $G=100$  kg/m<sup>2</sup>s and  $G=325$  kg/m<sup>2</sup>s at various heat fluxes.

Figure 4 illustrates that the effect of reducing vapor quality on the heat transfer coefficient depends on mass velocity. For  $G=100$  kg/m<sup>2</sup>s (see Fig. 4-a)) there is a negligible effect of decreasing  $x$  on the  $HTC$ , whereas for  $G=325$  kg/m<sup>2</sup>s (see Fig. 4-b)) a, apparently linear, reduction of the heat transfer coefficient with decreasing vapor quality is observed. Such behavior is related to a balance between gravitational and shear effects on the heat transfer coefficient, as similarly observed by Longo et al. (2019). At higher mass velocities the heat transfer is dominated by shear effects, being the heat transfer coefficient dependent on flow velocity. Therefore, associated with the reduction of vapor quality and, consequently, void fraction there is a decrease in the heat transfer coefficient, as noticed in Fig. 4-b). At low mass velocities the heat transfer is dominated by gravitational effects. Under these conditions, the  $HTC$  is unaffected by

changes in flow velocity, being independent of quality, as verified in Fig. 4-a) for  $G=100 \text{ kg/m}^2\text{s}$ . Figure 4 also displays a negligible effect of heat flux on the heat transfer coefficient regardless of mass velocity and vapor quality.

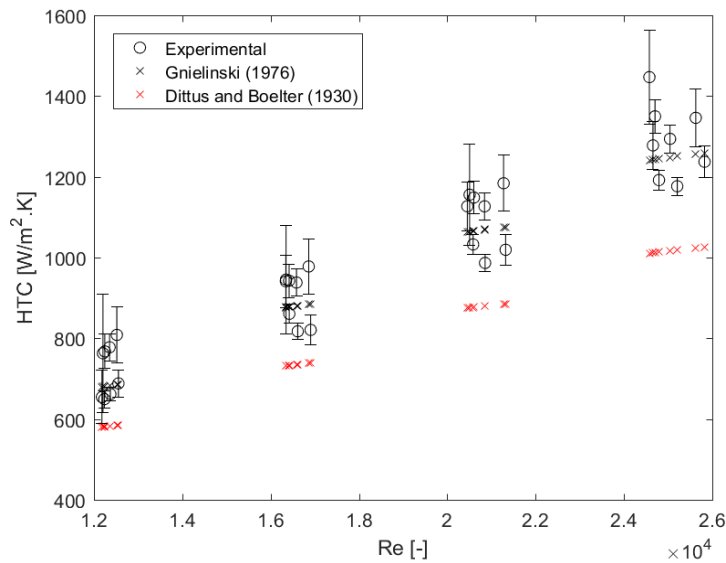


Figure 3. Experimental and predicted single-phase flow heat transfer coefficients with varying Reynolds number

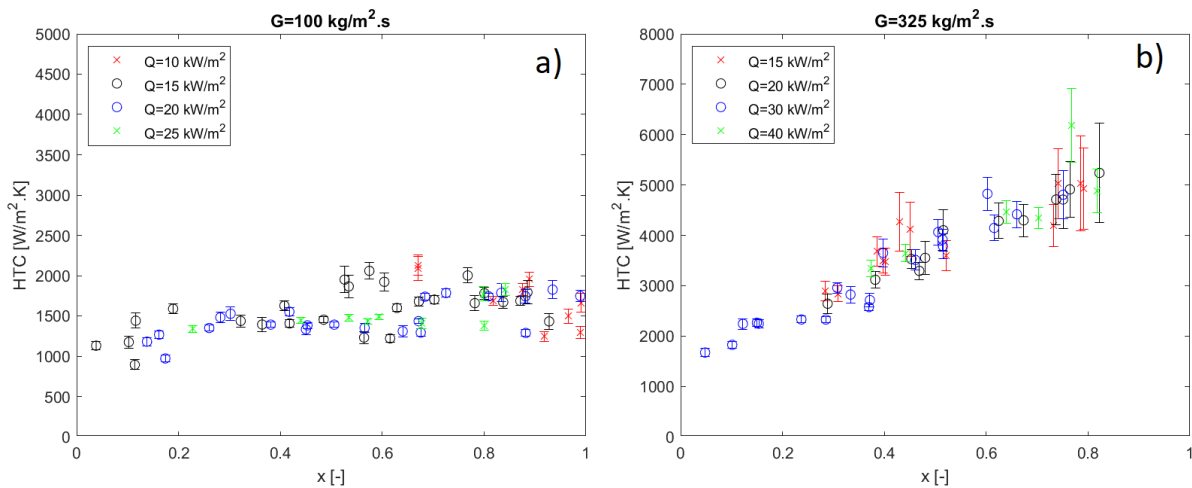


Figure 4.  $HTC$  with varying vapor quality for a)  $G=100 \text{ kg/m}^2\text{s}$  and b)  $G=325 \text{ kg/m}^2\text{s}$  at various heat fluxes.

Figure 5 depicts that the heat transfer coefficient increases with increasing mass velocity, behavior more pronounced as vapor quality increases. Indeed, at low qualities,  $x < 0.2$ , the effect of mass velocity becomes practically negligible. Such behavior is also related to the balance between gravitational and shear effects. At  $G=100 \text{ kg/m}^2\text{s}$ , the heat transfer is gravity-controlled, as above-mentioned, however, as mass velocity increases an increment of the relevance of shear effects relative to gravitational ones occurs, causing the increment of the heat transfer coefficient with increasing  $G$  verified in Fig. 5. With the increase of shear effects as mass velocity increases, changes in flow velocity affects more hardly the heat transfer coefficient, causing the  $HTC$  increment with  $G$  to reduce as  $x$  diminishes.

The experimental data was compared against twenty prediction methods from literature. Table 1 indicates statistical parameters ( $\psi$ , mean absolute deviation;  $\gamma_{20\%}$ , percentage of data predicted within an error band of  $\pm 20\%$ ) resulted from such comparison. As noticed in Tab. 1, in general, reasonable predictions of the heat transfer coefficient were obtained. The methods of Cavallini and Zecchin (1974), Shah (1979), Haraguchi et al. (1994), Tandon et al. (1995), Moser et al. (1998), Thome et al. (2003), Cavallini et al. (2006) and Shah et al. (2009) predicted the database with  $\psi < 20\%$  and  $\gamma_{20\%} > 70\%$ . Based on these results, although the most accurate predictions were obtained by the method of Cavallini and Zecchin (1974), a strictly empirical one, flow pattern-based methods provided the best overall results.

Figure 6 illustrates the comparison among the trend of experimental  $HTC$  as function of vapor quality and prediction methods that showed  $\psi < 20\%$  and  $\gamma_{20\%} > 70\%$ . In this figure it is observed that methods underpredicted the data for the

highest mass velocity and  $x > 0.5$ . Figure 6 also presents the flow pattern-based prediction method by Thome et al. (2003) as the one with the best overall results considering all mass velocities. The methods of Cavallini and Zecchin (1974) and Tandon et al. (1995) presented also reasonable predictions of the  $HTC$  trends with varying vapor quality. For the method of Cavallini and Zecchin (1974) the only exception is for  $G=100 \text{ kg/m}^2\text{s}$  and low vapor qualities. It is worth to highlight that this method is strictly empirical and developed for shear-dominated convective condensation, while in such conditions ( $G=100 \text{ kg/m}^2\text{s}$ ) the flow is gravity-driven, as discussed previously. The flow pattern-based method by Tandon et al. (1995) overpredicted the data for  $G=100 \text{ kg/m}^2\text{s}$  and  $x > 0.6$  and underpredicted for the other mass velocities at vapor qualities lower than 0.2.

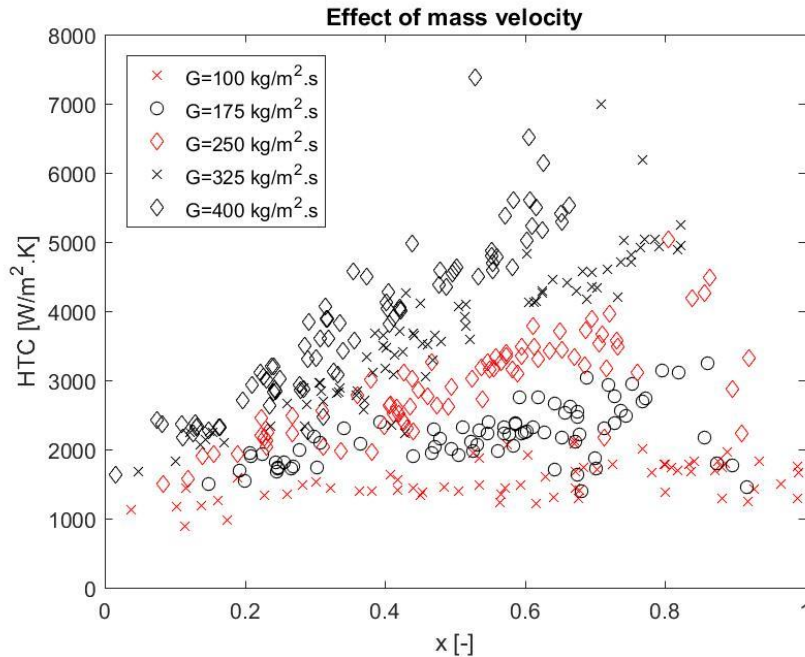


Figure 5. Effect of mass velocity on the  $HTC$ .

Table 1. Statistical parameters resulting from comparisons of the heat transfer coefficient and prediction methods.

Prediction method	$\psi$ (%)	$\gamma_{20\%}$ (%)
Akers et al. (1959)	26.5	41.9
Soliman et al. (1968)	17.3	64.8
Traviss et al. (1973)	27.1	63.5
Cavallini and Zecchin (1974)	11.9	85.2
Jaster and Kosky (1976)	34.4	24.2
Shah (1979)	14	78.4
Haraguchi et al. (1994)	14	82.3
Tandon et al. (1995)	18.1	70
Moser et al. (1998)	15.1	74.2
Dobson and Chato (1998)	18	59.4
Chang et al. (2000)	29.3	14.8
Zhang and Webb (2001)	30.7	12.2
Wang et al. (2002)	47.3	5.7
Jung et al. (2003)	50	33.6
Koyama et al. (2003)	51.8	22.4
Thome et al. (2003)	13.5	82.3
Cavallini et al. (2006)	17.1	70
Shah (2009)	16.9	75.8
Kim and Mudawar (2013)	51.8	46.6
Macdonald and Garimella (2016b)	30.7	13

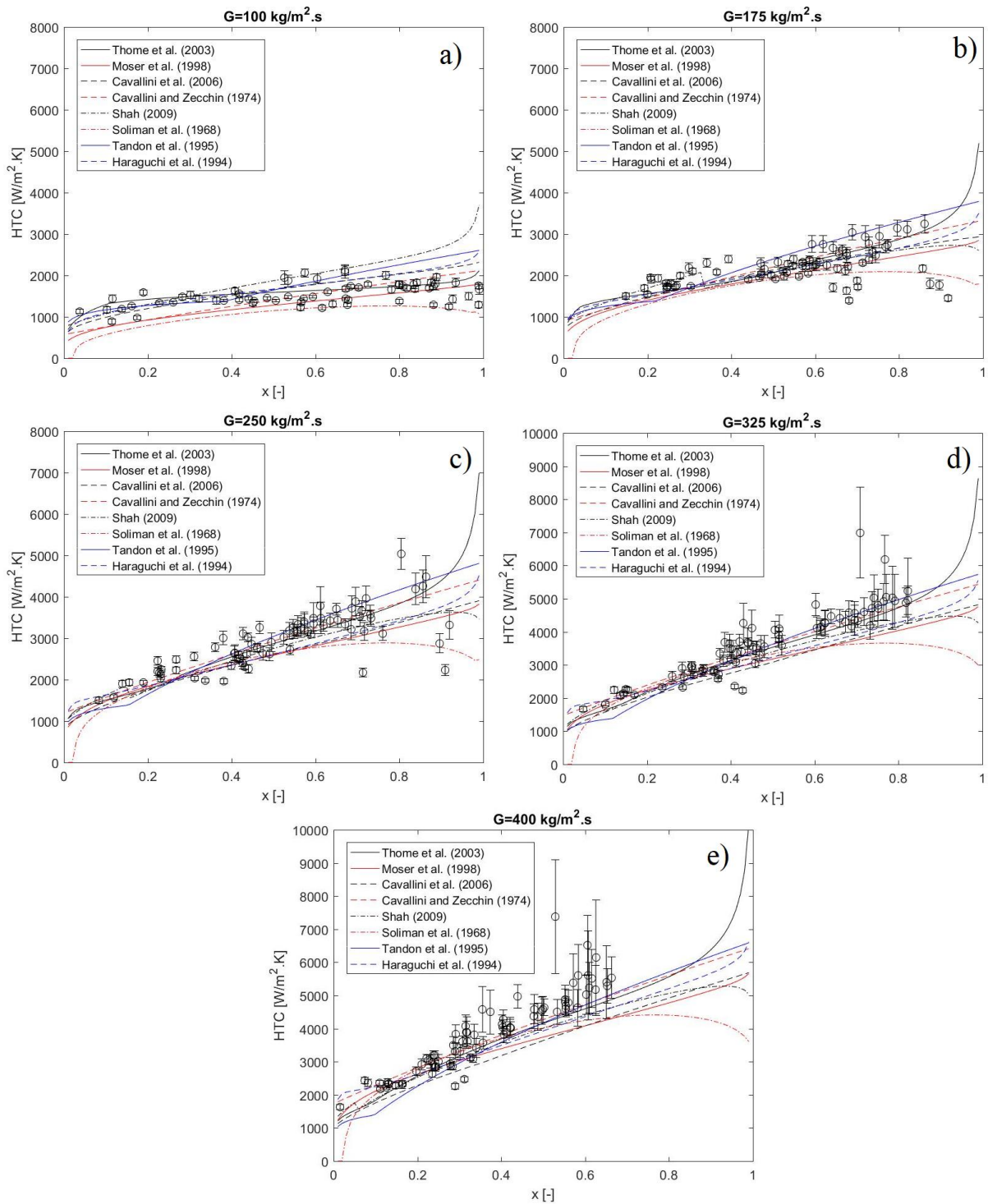


Figure 6. Comparison among the experimental and predicted  $HTC$  trend with varying vapor quality.

#### 4. CONCLUSIONS

Experiments for the convective condensation heat transfer coefficient of R134a inside a horizontal tube were performed for mass velocities ranging from 100 to 400  $\text{kg/m}^2 \cdot \text{s}$ , heat fluxes from 10 to 40  $\text{kW/m}^2$  and vapor qualities up to unity. The results indicated an increase of the heat transfer coefficient with increasing mass velocity, behavior more pronounced as the vapor quality, i. e. shear effects, increases. Except for  $G=100 \text{ kg/m}^2 \cdot \text{s}$ , the  $HTC$  reduces as vapor quality diminishes for all mass velocities. At the lowest mass velocity, the heat transfer is gravity-controlled regardless of vapor quality, therefore, the  $HTC$  is unaffected by changes in  $x$ . The experimental data were compared against twenty prediction methods. Reasonable agreement ( $\psi < 20\%$  and  $\gamma_{20\%} > 70\%$ ) between the experimental and predicted  $HTCs$  was

obtained for eight of them, with the best statistical results being given by the method of Cavallini and Zecchin (1974) and the most consistent trends with varying vapor quality by the method of Thome et al. (2003).

## 5. ACKNOWLEDGEMENTS

The authors acknowledge the CNPq (National Council for Scientific and Technological Development, Brazil) for the grant given under Contract Number 305673/2017-3, and FAPESP (São Paulo Research Foundation, Brazil) for the scholarships under Contract Numbers 2016/16849-3 and 2018/06057-4. Also, this study was financed in part by the Coordenação de Aperfeiçoamento de Pessoal de Nível Superior - Brasil (CAPES) - Finance Code 001.

## 6. REFERENCES

- Abernethy, R.B., Thompson, J.W., 1973. *Handbook of uncertainty in gas turbine measurements*. National Technical Information Service.
- Akers, W.W., Deans, H.A., Crosser, O. K., 1959. "Condensing heat transfer within horizontal tubes". *Chemical Engineering Progress Symposium Series*, Vol. 55, pp. 171–176.
- Ayub, Z. H., Ayub, A. H., Ribatski, G., Moreira, T. A., Khan, T. S., 2017. "Two-phase pressure drop and flow boiling heat transfer in an enhanced dimpled tube with a solid round insert". *International Journal of Refrigeration*, Vol. 75, pp. 1–13.
- Cavallini, A., Zecchin, R., 1974. "A dimensionless correlation for the heat transfer in forced convection condensation". *Proceedings of the "Fifth International Heat Transfer Conference"*, Vol. 3, pp. 309–313.
- Cavallini, A., Del Col, D., Doretti, L., Matkovic, M., Rossetto, L., Zilio, C., Censi, G., 2006. "Condensation in horizontal smooth tubes: a new heat transfer model for heat exchanger design". *Heat Transfer Engineering*, Vol. 27, pp. 31–38.
- Chang, Y., Kim, M., Ro, S., 2000. "Performance and heat transfer characteristics of hydrocarbon refrigerants in a heat pump system". *International Journal of Refrigeration*, Vol. 23, pp. 234–242.
- Del Col, D., Bortolin, S., Cavallini, A., Matkovic, M., 2011. "Effect of cross sectional shape during condensation in a single square minichannel". *International Journal Heat and Mass Transfer*, Vol. 54, pp. 3909–3920.
- Dittus, F.W., Boelter, L.M.K., 1930. "Heat transfer in automobile radiators of tubular type". *International Chemical Engineering*, Vol. 2, pp. 443–461.
- Dobson, M.K., Chato, J. C., 1998. "Condensation in smooth horizontal tubes". *Journal of Heat Transfer*, Vol. 120, pp. 193–203.
- Fries, S., Skusa, S., Luke, A., 2018. "Heat transfer and pressure drop of condensation of hydrocarbons in tubes". *Heat and Mass Transfer*, Vol. 55, pp. 33–40.
- Gnielinski, V., 1976. "New equations for heat and mass transfer in turbulent pipe and channel flow". *International Chemical Engineering*, Vol. 16, pp. 359–368.
- Haraguchi, E., Koyama, H., Fujii, H., 1994. "Condensation of Refrigerant HCFC-22, HFC-134a and HCFC-123 in a horizontal smooth tube". *Transactions of the JSME*, Vol. 60, pp. 2117–2126.
- Jaster, H., Kosky, P., 1976. "Condensation heat transfer in a mixed flow regime". *International Journal Heat and Mass Transfer*, Vol. 19, pp. 95–99.
- Jung, D., Song, K.H., Cho, Y., Kim, S.J., 2003. "Flow condensation heat transfer coefficients of pure refrigerants". *International Journal of Refrigeration*, Vol. 26, pp. 4–11.
- Kanizawa, F.T., 2011. *Estudo teórico e experimental sobre padrões de escoamento e perda de pressão durante escoamentos monofásicos e bifásicos no interior de tubos com fitas retorcidas*. Ph.D. thesis, Sao Carlos School of Engineering – University of Sao Paulo, Sao Carlos, Brazil.
- Kanizawa, F.T., 2011. *Estudo teórico e experimental sobre padrões de escoamento e perda de pressão durante escoamentos monofásicos e bifásicos no interior de tubos com fitas retorcidas*. Ph.D. thesis, Sao Carlos School of Engineering – University of Sao Paulo, Sao Carlos, Brazil.
- Kim, S. M., Mudawar, I., 2013. "Universal approach to predicting heat transfer coefficient for condensing mini/micro-channel flow". *International Journal Heat and Mass Transfer*, Vol. 56, pp. 238–250.
- Koyama, S., Kuwahara, K., Nakashita, K., Yakamoto, R., 2003. "An experimental study on condensation of refrigerant R134a in a multi-port extruded tube". *International Journal of Refrigeration*, Vol. 24, pp. 425–432.

- Kuehn, T.H., Ramsey, J.W., Threkeld, J.L., 1998. *Thermal Environmental Engineering*. 3<sup>rd</sup> ed. Prentice-Hall.
- Longo, G.A., Mancin, S., Righetti, G., Zilo, C., 2017. “Saturated condensation of HFC404A inside a 4 mm ID horizontal smooth tube: Comparison with the long-term low GWP substitutes HC290 (propane) and HC1270 (propylene)”. *International Journal Heat and Mass Transfer*, Vol. 108, pp. 2088–2099.
- Longo, G.A., Mancin, S., Righetti, G., Zilo, C., 2019. “Saturated vapour condensation of R134a inside a 4 mm ID horizontal smooth tube: Comparison with the low GWP substitutes R152a, R1234yf and R1234ze(E)”. *International Journal Heat and Mass Transfer*, Vol. 133, pp. 461–473.
- Macdonald, M., Garimella, S., 2016a. “Hydrocarbon condensation in horizontal smooth tubes: Part I – Measurements”. *International Journal Heat and Mass Transfer*, Vol. 93, pp. 75–85.
- Macdonald, M., Garimella, S., 2016b. “Hydrocarbon condensation in horizontal smooth tubes: Part II – Heat transfer coefficient and pressure drop modelling”. *International Journal Heat and Mass Transfer*, Vol. 93, pp. 1248–1291.
- Mogaji, T.S., 2014. *Theoretical and experimental study on convective boiling inside tubes containing twisted-tape inserts*. Ph.D. thesis, Sao Carlos School of Engineering – University of Sao Paulo, Sao Carlos, Brazil.
- Moser, K.W., Webb, R.L., Na, B., 1998. “A new equivalent Reynolds number model for condensation in smooth tubes”. *Journal of Heat Transfer*, Vol. 120, pp. 410–417.
- Sempertégui-Tápia, D.F.; Ribatski, G., 2017. “Flow boiling heat transfer of R134a and low GWP refrigerants in a horizontal micro-scale channel”. *International Journal Heat and Mass Transfer*, Vol. 108, pp. 2417–2432.
- Shah, M.M., 1979. “A general correlation for the heat transfer during film condensation inside pipes”. *International Journal Heat and Mass Transfer*, Vol. 22, pp. 547–556.
- Shah, M.M., 2009. “An improved and extended general correlation for heat transfer during condensation in plain tubes”. *HVAC&R Research*, Vol. 15, pp. 889–913.
- Soliman, H.M., Schuster, J.R., Bereson, P. J., 1968. “A general heat transfer correlation for annular flow condensation”. *Journal of Heat Transfer*, Vol. 90, pp. 167–176.
- Tandon, T., Varma, H., Gupta, C., 1995. “Heat transfer during forced convection condensation inside horizontal tube”. *International Journal of Refrigeration*, Vol. 18, pp. 210–214.
- Taylor, B. N., Kuayt, E. C., 1994. *Guidelines for evaluating and expressing the uncertainty of NIST measurement results*, National Institute of Standards and Technology (NIST), Technical note 1297.
- Thome, J. R., El Hajal, J., Cavallini, A., 2003. “Condensation in horizontal tubes. Part 2: new heat transfer model based on flow regimes”. *International Journal Heat and Mass Transfer*, Vol. 46, pp. 3365–3387.
- Traviss, D.P., Rohsenow, W.M., Baron, A.B., 1973. “Forced convection condensation inside tubes: a heat transfer equation for condenser design”. *ASHRAE Transactions*, Vol. 79, pp. 157-165.
- Wang, W.W., Radcliff, T.D., Christensen, R.N.A., 2002. “Correlation of two-phase friction for refrigerants in small-diameter tubes”. *Experimental Thermal and Fluid Science*, Vol. 26, pp. 473-485.
- Zhang, M.; Webb, R.L., 2001. “Correlation of two-phase friction for refrigerants in small-diameter tubes”. *Experimental Thermal and Fluid Science*, Vol. 25, pp. 131-139.

## 7. RESPONSIBILITY NOTICE

The authors are the only responsible for the printed material included in this paper.